Extended Abstract for Plenary Lecture, 16th International Conference on Nucleation and Atmospheric Aerosols, Kyoto, Japan, July 26-30, 2004; Draft March 15, 2004

Aerosols, Clouds, and Climate Change

Stephen E. Schwartz

Brookhaven National Laboratory
Upton NY 11973 USA

Abstract. Earth's climate is thought to be quite sensitive to changes in radiative fluxes that are quite small in absolute magnitude, a few watts per square meter, and in relation to these fluxes in the natural climate. Atmospheric aerosol particles exert influence on climate directly, by scattering and absorbing radiation, and indirectly by modifying the microphysical properties of clouds and in turn their radiative effects and hydrology. The forcing of climate change by these indirect effects is thought to be quite substantial relative to forcing by incremental concentrations of greenhouse gases, but highly uncertain. Quantification of aerosol indirect forcing by satellite- or ground-based remote sensing has proved quite difficult in view of inherent large variation in the pertinent observables such as cloud optical depth, which is controlled mainly by liquid water path and only secondarily by aerosols. Limited work has shown instances of large magnitude of aerosol indirect forcing, with local instantaneous forcing upwards of 50 W m^{-2}. Ultimately it will be necessary to represent aerosol indirect effects in climate models to accurately identify the anthropogenic forcing at present and over secular time and to assess the influence of this forcing in the context of other forcings of climate change. While the elements of aerosol processes that must be represented in models describing the evolution and properties of aerosol particles that serve as cloud condensation particles are known, many important components of these processes remain to be understood and to be represented in models, and the models evaluated against observation, before such model-based representations can confidently be used to represent aerosol indirect effects in climate models.

Key Words: Aerosols, Clouds, Climate, Radiative forcing

INTRODUCTION

We are meeting in Kyoto, a city whose name has become epynomous with the issue of climate change. The issue that we confront, as citizens of the world, is how to respond to the consequences of inevitable increases in atmospheric carbon dioxide associated with fossil fuel combustion. Briefly the options are mitigation (reductions in CO_2 emissions, which can take place only at considerable cost to our energy economy) and adaptation (preparation to live in a greenhouse warmed world, also at great social cost). Our responsibility, as scientists, is to develop improved understanding of Earth's climate system, so that we may be able to state with confidence the nature and extent of climate change that would result from prospective perturbations to the climate system.

If we have learned anything in the study of climate it is that there is a potential of large changes in climate from small changes in radiative fluxes. The global- and annual-average increase in downwelling irradiance at the tropopause from a doubling of CO_2 (which seems inevitable in the lifetime of many alive today) is roughly 4 W m^{-2}. This perturbation in one of the key radiative flux components of Earth's climate system, a so-called radiative forcing of climate change, is usefully compared with the flux itself, ~325 W m^{-2} (Ramanathan, 1987; Kiehl and Trenberth, 1997), or hardly more than 1%. According to present understanding, as summarized in the 2001 assessment report of the Intergovernmental Panel on Climate Change (IPCC, 2001) such a slight radiative forcing would result in an increase in global mean temperature of 3 ± 1.5 K (IPCC). Such a change is again of order 1%, but such a global temperature change must be reckoned as potentially quite a serious perturbation to Earth's climate, given the fact that the difference between the present global mean temperature and that in the last glacial ice age is 6 K (Folland *et al*., 2001). Perhaps just as important for decision

making is the uncertainty in the estimated temperature increase; a global mean temperature increase of 1.5 K would be of much less consequence to society than an increase of 4.5 K. Determining Earth's climate sensitivity, the change in global mean temperature that would result from a given forcing, is thus a major objective of present research on climate change.

A key assumption underlying the climate sensitivity concept is that the global mean temperature change over a suitably long averaging period is proportional to the totality of changes in global mean radiative fluxes over that period. This radiative forcing hypothesis is the basis for comparisons of magnitudes and uncertainties in radiative forcing of climate change over the industrial period. Central to the quantitative understanding of climate change over this period, whether through the use of global climate models or by empirical inference, is the need to know, with sufficient accuracy, the total forcing over this period.

In its 2001 assessment the IPCC identified the key contributors to radiative forcing of climate change and provided estimates of the magnitudes and uncertainties of these forcings, as shown in Figure 1. In addition to forcings due to changes in concentrations of long- and short-lived greenhouse gases (GHGs) the IPCC identified forcings due to light scattering and absorption by aerosols in clear (cloud-free) air and changes in cloud microphysical properties

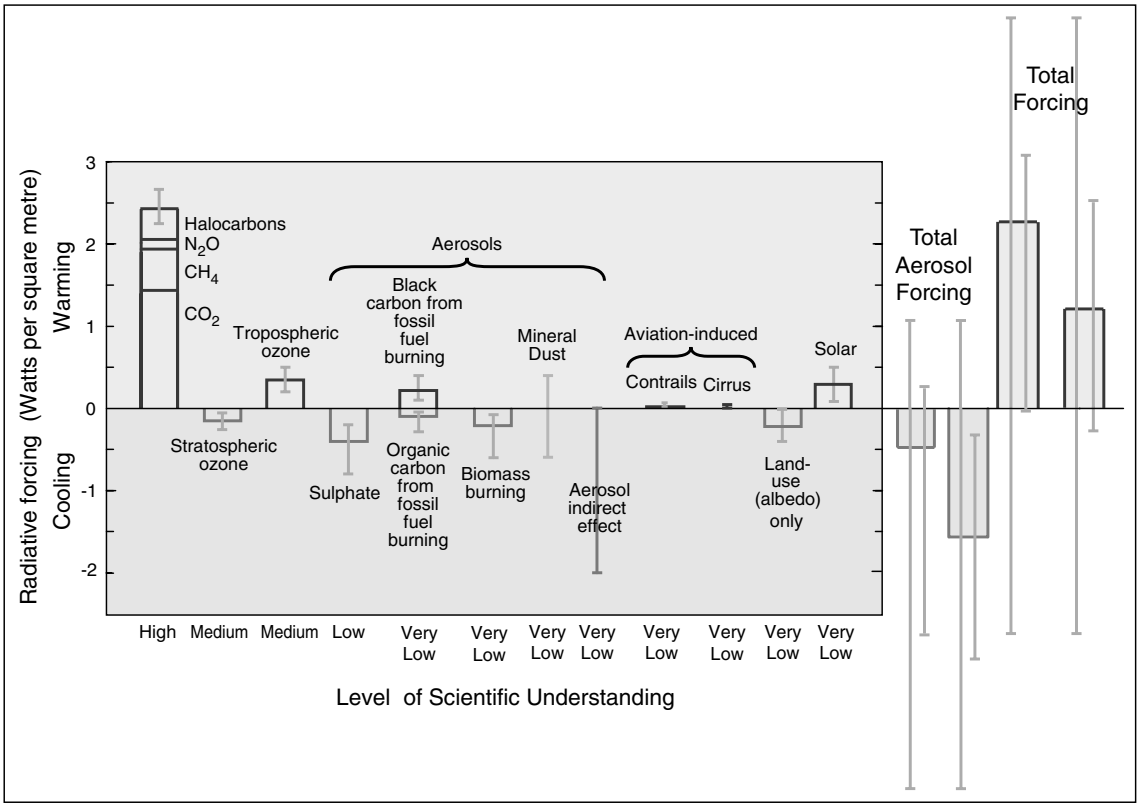

Figure 1. Global mean radiative forcing of climate change for the year 2000 relative to 1750 as given by the Intergovernmental Panel on Climate Change (2001), shown in the left portion of the figure. Positive bars denote warming forcings; negative bars denote cooling forcings; I-beams denote estimated uncertainties. For mineral dust and the aerosol indirect effect no estimates of the forcing were given, only uncertainty ranges. Level of scientific understanding represents the subjective judgment of the IPCC working group on radiative forcing of the reliability of the forcing estimate. Bars and I-beams at right denote estimates of total aerosol forcing, total forcing, and associated uncertainties. First bar denotes total aerosol forcing evaluated as algebraic sum of IPCC aerosol forcings, with mineral dust and aerosol indirect forcings taken as zero; for second bar these forcings are taken as the mid-points of the IPCC uncertainty ranges. Third and fourth bars denote total forcing evaluated in the same way, again with mineral dust and aerosol indirect forcings taken as zero and as the mid-points of the IPCC uncertainty ranges, respectively. For each bar two uncertainty estimates are provided. Upper and lower limits of the first (larger) uncertainty range are calculated as algebraic sum of upper and lower limits, respectively, of the uncertainties of the several forcings. Upper and lower limits of the second (smaller) uncertainty range are calculated as square root of the sum of the squares, respectively, of the upper and lower uncertainty ranges relative to the estimated forcings denoted by the bars.

by aerosols as key contributors to radiative forcing of climate change, most likely exerting a cooling influence but of highly uncertain magnitude. If the total aerosol forcing is negative, that is exerting a cooling influence, then this aerosol forcing would be offsetting a fraction, perhaps a substantial fraction, of the warming forcing due to increased concentrations of GHGs. Importantly in the context of this conference on atmospheric aerosols these aerosol induced forcings are considered the greatest source of uncertainty in the totality of radiative forcing over the industrial period. The present uncertainties in aerosol forcing preclude accurate assessment of the total forcing over the industrial period; the total forcing over the industrial period might be substantially lower (or greater) than the forcing due to GHGs alone (Boucher and Haywood, 2002; Gregory, 2002). For a given amount of warming over the industrial period, a lower (greater) forcing would imply a greater (lower) climate sensitivity, (Gregory, 2002).

Of the several aerosol forcings identified, the so-called indirect forcing, arising from the influence of anthropogenic aerosols on the microphysical, optical, and radiative properties of clouds is considered to be the most uncertain. As a consequence of this uncertainty the IPCC panel declined to provide an estimate of this forcing, indicating, rather, a likely range (0 to -2 W m^{-2}). This uncertainty range is quite wide relative to both the magnitude and uncertainty of forcing by the long-lived GHGs (+2.45 ± 0.4 W m^{-2}). As the uncertainty in aerosol forcing dominates the uncertainty in the total radiative forcing of climate change over the industrial period, as indicated by the uncertainties indicated on the total forcing at the right-hand side of Figure 1, the uncertainty in aerosol forcing assumes a major importance in understanding and quantifying climate change over the industrial period. It is thus clear that quantification of this forcing must be greatly improved if the uncertainty in forcing, and hence in climate sensitivity, is to be substantially reduced.

Two approaches seem available to identifying indirect forcing and quantifying it on climatologically relevant scales–observational and modeling–but neither is entirely straightforward. Suppose it proved possible to determine cloud albedo by satellite measurements with sufficient global coverage to be representative: how then might one identify and quantify the anthropogenic enhancement? The alternative approach, first-principles modeling would seem intellectually satisfying, but there are many gaps in present understanding of the pertinent processes and consequently large modeling uncertainties.

This presentation examines present knowledge and some new developments in the understanding of aerosol indirect forcing of climate change and points to some important future directions.

PHYSICAL BASIS OF INDIRECT FORCING

While influences of anthropogenic aerosols on cloud properties and precipitation development had been recognized for some time, it was the seminal work of Sean Twomey in the 1970s (Twomey, 1974) that first called attention to the possible climatic influence through the mechanism of increased cloud droplet number concentration (CDNC) and resultant enhancement of cloud reflectivity, now commonly referred to as the "first indirect aerosol effect" or often the "Twomey effect." This effect is manifested as an enhancement in cloud-top reflectivity associated with an increase in CDNC at a given cloud physical thickness under assumption of fixed cloud liquid water content, Figure 2. The assumption of fixed liquid water content is based on the assumption that this liquid water content is governed by thermodynamics and would not be expected to hold under conditions in which water has been appreciably removed from the cloud by precipitation. For clouds of intermediate optical depth the enhancement in cloud-top reflectance and resultant radiative forcing can be substantial for even a slight increase in CDNC. The magnitude of this effect can be illustrated in a number of ways. Figure 3 shows that the enhancement of cloud-top reflectance, local top-of-atmosphere reflectance, and global-average top-of-atmosphere reflectance and the resultant global-average shortwave radiative forcing increase linearly with the logarithm of the ratio of the cloud droplet number concentration in the anthropogenically perturbed situation to that in the unperturbed situation. In view of the nonlinearity of the forcing and nonuniform perturbations in CDNC,

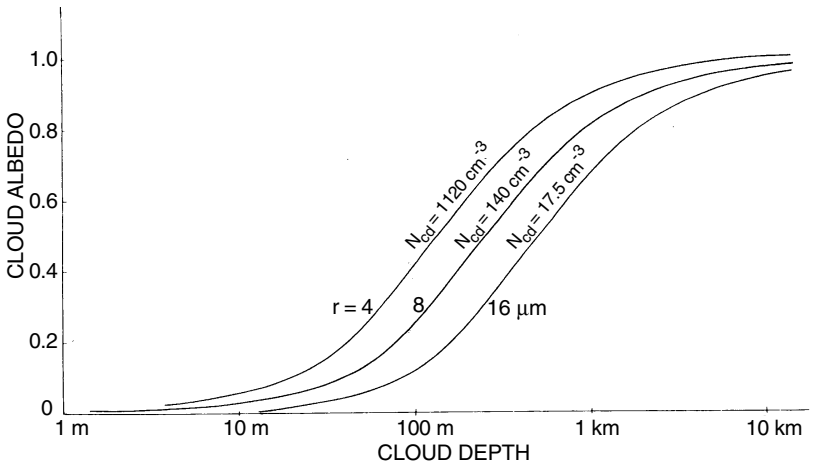

Figure 2. Dependence of cloud-top albedo on cloud thickness and indicated values of cloud droplet radius r and number concentration N_{cd}. Liquid water content, 0.3 cm^3 m^{-3}; asymmetry parameter, 0.858. Modified from Twomey (1977).

suitable averaging would be required. Nonetheless the figure demonstrates the very high sensitivity of the forcing to perturbation in CDNC; an increase in CDNC in marine stratus clouds globally of only 30% would result in a radiative forcing of about -1 W m^{-2}. A forcing of this magnitude was estimated (Charlson *et al.*, 1992) based on an estimated 30% enhancement of aerosol sulfate mass loading, relative to natural non seasalt sulfate. Of course such an estimate neglects the important role of other aerosol species, both natural and anthropogenic, which might increase or diminish the indirect forcing.

Numerous in-situ studies have shown that at least locally, concentrations of aerosol particles that might serve as cloud condensation nuclei (CCN) are greatly enhanced, by an order of magnitude or more, over their natural abundances because of anthropogenic emissions; see Figure 4 and the summaries by Leaitch *et al.* (1986), Schwartz and Slingo (1996) and Chuang *et al.* (2000). Likewise cloud drop concentrations in anthropogenically influenced clouds are also substantially enhanced over the concentrations in clouds that are not influenced by anthropogenic emissions. Such studies suggest substantial resultant enhancement of cloud albedo. The rather great spatial and temporal variability of anthropogenic enhancement of aerosol particle concentrations suggests a similar variability in cloud albedo that might guide identification and quantification of these influences.

In addition to the influence of enhanced concentrations of aerosol particles on cloud albedo, enhanced particle concentrations are also thought to inhibit development of precipitation, resulting in more persistent clouds with resultant additional cooling influence, the so-called second indirect aerosol forcing (Albrecht, 1989). Yet another aerosol indirect effect has been postulated, in which a broadening of cloud drop size distribution (for constant liquid water content and CDNC) would result in a decrease of cloud albedo (Liu and Daum, 2002).

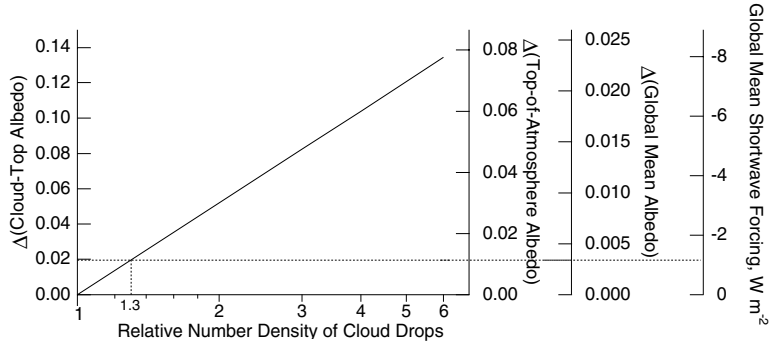

Figure 3. Calculated relation between albedo and cloud droplet number concentration N_{cd}. The sloping line shows the relation between the albedo (at various levels of the atmosphere and globally) as a function of an increase in N_{cd}. The four ordinates show the perturbation in cloud-top albedo (left axis), TOA albedo above marine stratus (first right axis), global-mean albedo (second right axis), and global-mean cloud radiative forcing (far right axis). The fractional atmospheric transmittance of short-wave radiation above the cloud layer was taken as 76%. The dotted line indicates the perturbations resulting from a 30% increase in N_{cd} (after Charlson *et al.*, 1992).

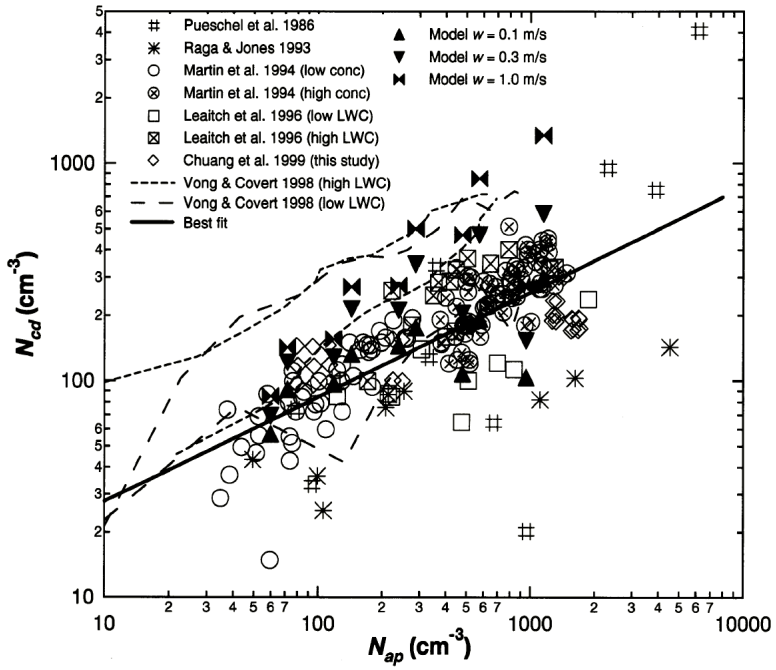

Figure 4. Summary (Chuang *et al.*, 2000) of measurements of the relation between number concentration of cloud droplets N_{cd} and below- or in-cloud accumulation mode aerosol particles N_{ap}. Lines for the Vong and Covert (1998) data represent the envelope of their data (for high and low liquid water content cases). Best-fit line (slope 0.48) is regression of all measurements except for the Vong and Covert data. The model data D1 and D2 represent results of Chuang *et al.* (2000) for two size distributions. Reprinted from *Tellus* **52B** 843-847 (2000). Permission pending.

QUANTIFYING INDIRECT FORCING IN REMOTE SENSING

Several studies have attempted to identify indirect forcing by anthropogenic aerosols using satellite remote sensing data. An important early study was that of Han *et al.* (1994), which compared zonal mean cloud drop effective radius r_e (ratio of third to second moment of the cloud drop size distribution, important for radiative transfer; Hansen and Travis, 1974), from AVHRR (Advanced Very High Resolution Radiometer) measurements in the Northern and Southern Hemispheres under the hypothesis that anthropogenic aerosols, predominantly in the Northern Hemisphere would lead to an enhancement of CDNC relative to the Southern Hemisphere and resultant decrease in cloud drop radius. Comparisons were made separately for continental and maritime clouds. Effective radii were smaller in the NH (average 11.6 μm for maritime clouds; 8.2 μm for continental clouds) than in the SH (12.0 μm and 9.0 μm, respectively), Figure 5. For fixed liquid water content, a decrease in effective radius by 3.4% and 10%, for maritime and continental clouds respectively, would correspond to an increase in CDNC by 10% and 30%, respectively, and might be expected to result in an enhancement in cloud-top albedo of 0.007 and 0.02, respectively. However subsequent examination by the same group (Han *et al.*, 1998) of interhemispheric differences in cloud albedo determined by the International Satellite Cloud Climatology Project (ISCCP) failed to reveal any systematic indication of aerosol influence. This was attributed to lack of constancy of cloud liquid water path as a function of cloud droplet size (Han *et al.*, 1998, 2002).

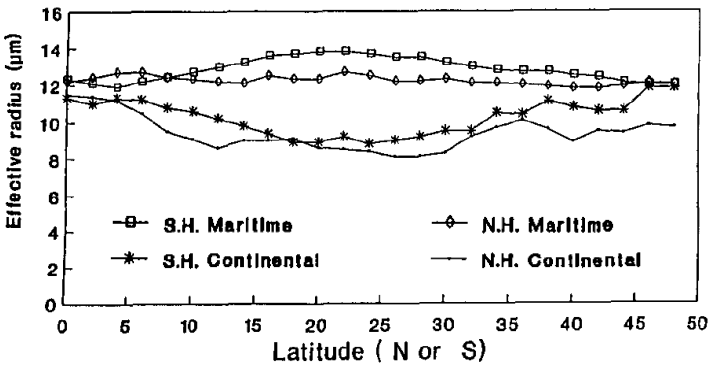

Figure 5. Annual (four-seasonal-month) average, zonal mean water cloud droplet effective radii for 1987 from analysis of NOAA-9 AVHRR radiances. From Han *et al.* (1994).

Several studies have attempted to identify and quantify aerosol indirect forcing in satellite-based sensing by examination of correlations between cloud albedo (or other microphysical properties) and proximate remotely sensed aerosol properties. Nakajima *et al.*, (2001) compared monthly-average cloud and clear-aerosol properties determined from AVHRR radiance measurements. Retrieved quantities included aerosol optical depth τ_c aerosol particle column number concentration N_a, cloud optical depth, cloud drop effective radius, and cloud drop column number concentration N_c. Taking advantage of the large spatial variation in these quantities they were able to adduce correlations among the several quantities, including a positive sublinear correlation of N_c with N_a, $\log_{10} N_c = (1.80 \pm 0.43) + (0.50 \pm 0.07)\log_{10} N_a$; here N_a and N_c are in particles cm^{-2}. Effective radius r_e decreased from about 15 μm at low N_a to about 12 μm at high N_a. Bréon *et al*. (2002) examined spatial correlation of monthly mean r_e with monthly mean aerosol index (a measure of aerosol loading) in data from the POLDER (POLarization and Directionality of the Earth's Reflectances) satellite-borne radiometer. Effective radius decreased with increasing aerosol index from about 11 μm (ocean) or 9 μm (land) to about 8 μm.

Indication of a remarkably strong aerosol influence on cloud albedo was found in an examination (Chameides *et al*., 2002) of correlation of cloud optical depth (from ISCCP) and modeled anthropogenic aerosol for China and neighboring regions, Figure 6. Values of R^2, the square of the Pearson product-moment correlation coefficient, were approximately 0.6 for correlation between modeled four-seasonal-month average (Nov. 1994; Jan., April, and July 1995) column mass burden of anthropogenic aerosol (sulfate, nitrate, ammonium organic carbon, other organic elements, and elemental carbon) and annual average (1993) low-cloud and total cloud optical depth and cloud amount. While such high correlations are indicative of coherent long-term average spatial patterns of aerosol concentration and cloud optical depth, it is not clear whether the high optical depth is causally related to the high aerosol loading or is merely a consequence of persistent clouds in this region of China north of the Tibetan plateau and high anthropogenic aerosol concentrations resulting from high emissions and persistent inversions in this region. What would seem to be required to ascribe enhancement of cloud optical depth to aerosols is analysis of short-term situations of comparable cloud liquid water but variable aerosol loading to see if the correlation persists.

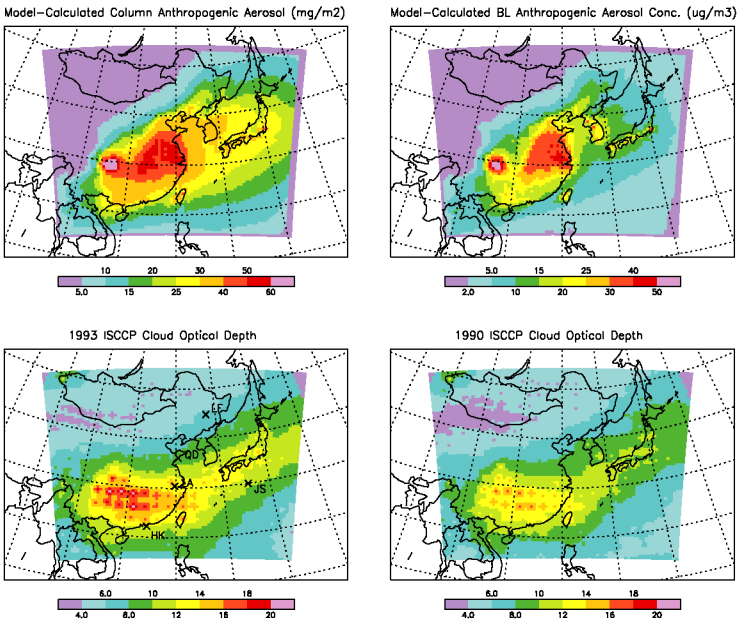

Figure 6. Four-month average (Nov. 1994; Jan., April, and July 1995) distributions of modeled column-integrated (top-left) and boundary-layer concentration (top-right) of anthropogenic aerosols, and annual-average ISCCP-derived total-cloud optical depth for 1993 (bottom-left) and 1990 (bottom-right). From Chameides *et al*. (2002).

An alternative approach, which thus far has seen only limited application is based on examination of temporal variation of cloud properties and aerosol loading in a region. A recent study by our group in collaboration with Harshvardhan of Purdue University (Harshvardhan *et al*., 2002; Schwartz *et al*., 2002) examined cloud properties determined from AVHRR radiance measurements in conjunction with output of a chemical transport model (Benkovitz *et*

al., 1994, 2001) to examine dependence of cloud properties on sulfate aerosol concentration. The study examined the time dependence of cloud properties in $5^\circ \times 5^\circ$ regions of the North Atlantic well removed from local sources during specific episodes of transport from North America or Europe during which sulfate concentrations increased and then decreased over several-day periods. The AVHRR measurements, which were each afternoon, local time, provide high resolution (1 km × 4 km) data of visible, near infrared, and thermal infrared irradiance. Only low clouds (cloud top temperatures greater than 260 K as determined from thermal infrared) were examined, and rigorous attention was given to exclusion of potentially inhomogeneous pixels by comparison of examined pixels with adjacent pixels. Following Nakajima and Nakajima (1995) we used visible and near infrared data to determine cloud drop effective radius and cloud visible optical depth τ_c. These measurements allowed determination of cloud liquid water path (LWP) as $L = (3/2)\rho_w \tau_c r_e$ where ρ_w is density of liquid water. In general we have found that LWP is highly variable spatially, presumably as a consequence of locally variable cloud dynamics. As a consequence cloud optical depth and cloud albedo are similarly highly variable. This variability undoubtedly limits ability to infer or quantify aerosol indirect effects from examination of cloud albedo. Examination on any given day of the dependence of cloud optical depth on LWP showed, not surprisingly, a strong dependence, as LWP is the dominant influence on cloud optical depth. It is possible to use this variation to advantage to identify day-to-day differences in effective radius from the slopes of a plots of optical depth versus LWP, that slope being inversely proportional to r_e. Comparison of the slopes of such plots over the course of the several-day episodes revealed substantial variation of effective radius, as illustrated in Figure 7 for an episode of transport of European sulfate to a location ~1200 km west of Ireland.

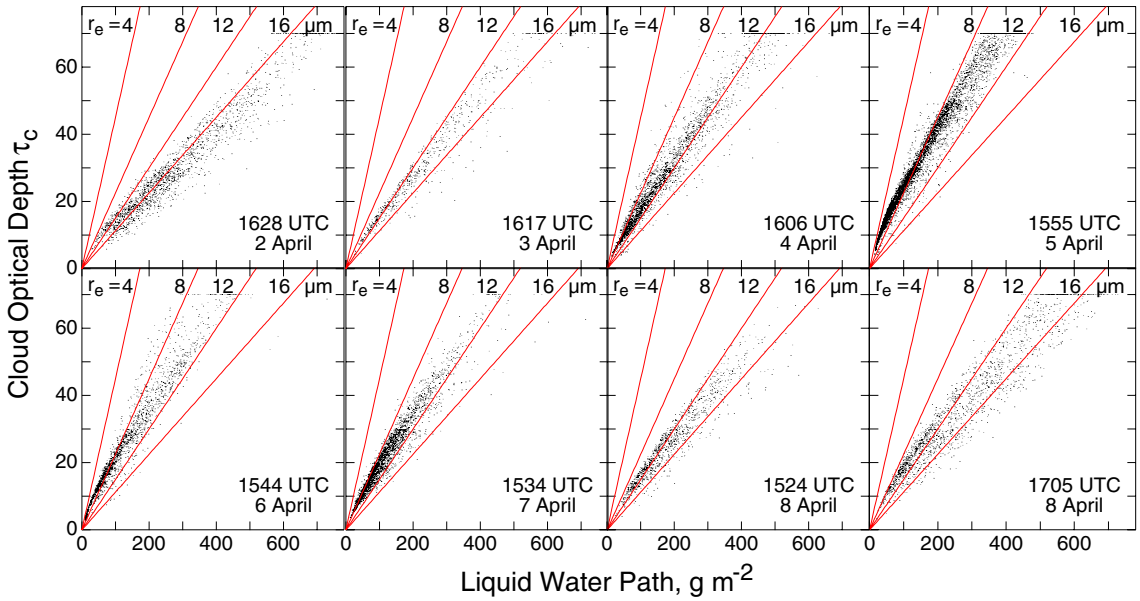

Figure 7. Pixel-average cloud optical depth τ_c as a function of vertical cloud liquid water path for eight satellite overpasses over a study area 50-55˚N, 25-30˚W, for April 2-8, 1987; two sets of data are shown for April 8, for which the study area was within range of the satellite on two successive overpasses. Data points with $\tau_c > 70$ are plotted at $\tau_c = 70$ because of insensitivity of retrieval method at high optical depth; these points are evident as horizontal clusters at $\tau_c = 70$. Data points with $\tau_c \lesssim 3$ were excluded to eliminate pixels that could be covered by haze but not clouds. Lines denote cloud optical depth for indicated constant values of effective radius r_e. From Schwartz *et al*. (2002).

The variation over the course of the episode of sulfate concentration and of several cloud properties derived from the satellite measurements, summarized in Figure 8, illustrates several important features of this data set. First the modeled sulfate column burden (vertical integral of concentration) exhibited a marked increase and then decrease over the course of the 6-day period. In contrast there was no evident trend in cloud optical depth or albedo derived from this optical depth, and on any given day these quantities can exhibit excursions throughout

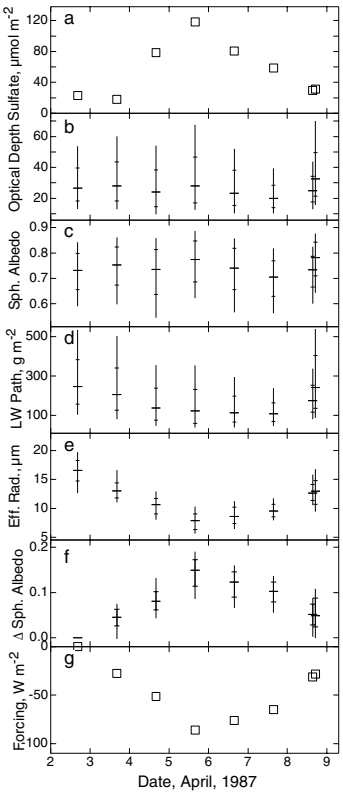

Figure 8. Time series of sulfate column burden from chemical transport model and pixel-average (1 km × 4 km) cloud properties determined from satellite retrievals over mid North Atlantic, 25-30˚W, 50-55˚N, April 2-8, 1987. *a*) Modeled sulfate column burden, obtained by interpolation of model output at 6-h intervals; *b*) optical depth, τ_c; *c*) cloud-top spherical albedo, α_{sph}; *d*) liquid water path, LWP; *e*) effective radius at cloud top, r_e; *f*) enhancement of cloud-top spherical albedo relative to that calculated for April 2 for the same LWP distribution; *g*) radiative forcing at top of atmosphere, relative to April 2, calculated for LWP = 100 g m^{-2} and solar zenith angle 60˚. Bars denote central 80% of the data; ticks note upper quartile, median, and lower quartile. Two sets of data are shown for April 8, for which the study area was within range of the satellite on two successive overpasses. Dates and times are UTC. From Schwartz *et al*. (2002).

most of the observational range of the entire data set. There was likewise considerable variation in LWP, although there is a discernible trend, actually, to increased LWP toward the middle of the episode; such a variation is likely under control of larger-scale dynamics rather than microphysics, as any inhibition of precipitation by incremental sulfate would result in an increase in LWP. In contrast there is a marked decrease in cloud drop effective radius that is coherent with the increase in sulfate, which would be consistent with the first indirect effect.

The influence of enhanced aerosol loading on cloud spherical albedo α_{sph} is examined in Figure 9. While the dominant influence on cloud albedo is LWP, marked day-to-day differences are readily apparent in graphs of cloud spherical albedo versus LWP. The clusters of data points for the several days are distinctly segregated, manifesting the different dependences on the several days. Also shown in the figure are curves representing the dependence of α_{sph} on LWP for specific values of cloud-top effective radius, r_e = 4, 8, and 16 μm. These curves, which may be directly compared to those given by Twomey (Figure 2 above), explicitly show the increase in modeled cloud albedo with decreasing drop radius for a given LWP. The aerosol influence is similarly manifested in the data by the points at a given LWP exhibiting a higher cloud albedo on days with higher aerosol loading. Thus, although the aerosol influence is not evident in comparisons of the aggregate cloud albedo for the several days (Figure 8*f*), at any given LWP cloud albedo was greater on April 5, at the peak of the sulfate incursion, than on April 7, toward the end of the episode, or on April 2, prior to the episode.

The enhancement in cloud albedo between the high sulfate, low r_e day (April 5) and the low sulfate, high r_e day prior to the episode (April 2) is shown in Figure 10, evaluated as the difference between α_{sph} calculated from τ_c and r_e obtained from satellite data for April 5 and α_{sph} calculated for the same LWP using a linear fit of τ_c to LWP for the April 2 data. This plot explicitly shows the amount by which α_{sph} has been enhanced over what it would have been with the same LWP but with r_e characteristic of the unperturbed day, consistent with the Twomey mechanism for albedo enhancement by anthropogenic aerosols. Plotting the enhancement against LWP shows the maximum enhancement at intermediate values of LWP, for which the sensitivity to increased cloud-drop number concentration is the greatest. The enhancement in α_{sph} relative to April 2 evaluated in this way for the entire episode (Figure 8*f*)

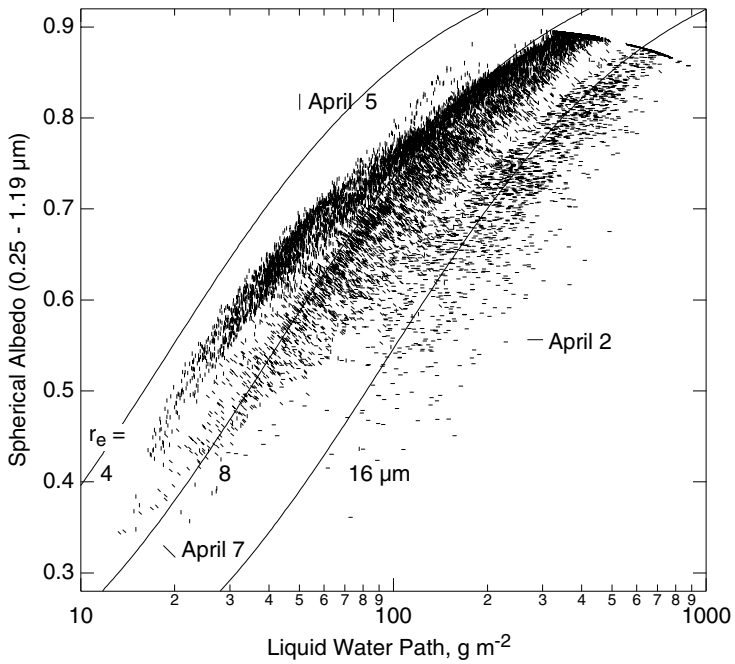

Figure 9. Pixel-average cloud spherical albedo as a function of vertical cloud liquid water path, for three satellite overpasses for the area 50-55˚N, 25-30˚W for the indicated dates in April, 1987. Clusters of points at albedo ~0.88 represent points with $\tau_c > 70$ for which spherical albedo was calculated as if $\tau_c = 70$. Curves denote cloud albedo for indicated constant values of effective radius r_e. From Schwartz *et al*. (2002).

mirrors the excursions in effective radius and sulfate over this period. The corresponding radiative forcing, calculated for a solar zenith angle of 60˚ and constant assumed LWP of 100 g m^{-2} (Figure 8*g)* approaches -85 W m^{-2} at the peak of the episode. While this calculation may be somewhat artificial in view of the assumed effective radius of the base case, 17 μm, and the constant LWP, it nonetheless establishes the magnitude of the first indirect forcing that may be experienced locally as a consequence of anthropogenic aerosol and high sensitivity of forcing to enhanced aerosol number concentration. Perhaps just as important, this study demonstrates the large day-to-day variation in cloud properties associated with variation in aerosol properties. Such variation would seem to call into question inferences of the magnitude of aerosol indirect effect based on spatial correlations alone.

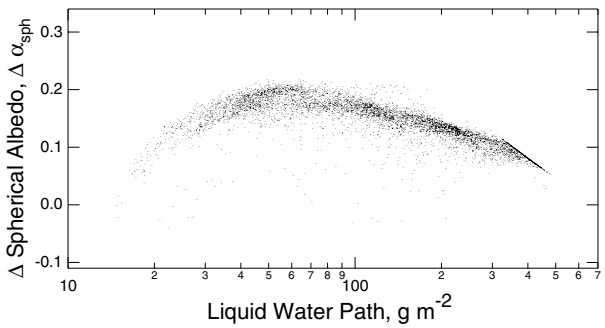

Figure 10. Enhancement of pixel-average cloud spherical albedo $\Delta\alpha_{sph}$ on April 5, 1987, relative to that on April 2, as a function of LWP, for 50-55˚N, 25-30˚W. $\Delta\alpha_{sph}$ was evaluated for each datum of April 5 as the difference between α_{sph} calculated using τ_c and r_e obtained from satellite data for that date and the value at the same LWP calculated using a linear fit of τ_c to LWP for April 2. Data points for $\tau_c > 70$ (592 data out of a total of 6443), calculated for $\tau_c = 70$, lie along the diagonal line at the upper right. From Schwartz *et al*. (2002).

An additional approach to remote sensing of the indirect aerosol effect is through ground-based remote sensing. Several groups (Min and Harrison, 1996; Dong *et al*, 1997; Feingold *et al*., 2003; Penner *et al*., 2004) have determined cloud microphysical properties through measurements of liquid water path (microwave radiometer) cloud optical depth (by sun photometry) and/or cloud drop radius (cloud radar). In our work (Kim *et al*., 2003) we have determined τ_c by narrow-band sun photometry at 415 nm, which minimizes sensitivity to surface reflectance. The method is limited to complete overcast conditions (indicated in part by coincidence of direct and total downwelling solar irradiance) because of photon diffusion in clouds as well as the wide field of view of the photometer. Cloud boundaries are determined by cloud radar. LWP is determined by microwave radiometry. An example of the primary data is given in Figure 11 for measurements at a site in north central Oklahoma. Cloud optical

depth is determined by a radiation transfer model (Ricchiazzi *et al*., 1998). Cloud optical depth is in turn approximately equal to twice the vertical integral of the square of the cloud drop radius integrated over the drop size distribution:

$$\tau_c = \iint \pi r^2 Q_e(r) N(r,z) dr dz \approx 2 \iint \pi r^2 N(r,z) dr dz \qquad (1)$$

where $Q_e(r)$, the extinction efficiency for a cloud droplet of radius r is equal to 2 within a few percent for cloud droplets of radius much greater than the wavelength of visible light. Similarly LWP is equal to $(4\pi/3)$ times the vertical integral of the cube of the cloud drop radius integrated over the drop size distribution:

$$L = \frac{4\pi}{3} \rho_w \int \int r^3 N(r,z) dr dz \qquad (2)$$

from which the effective radius pertinent to the cloud as a whole is calculated as

$$r_e = \frac{3}{2} \frac{L}{\rho_w \tau_c} . \qquad (3)$$

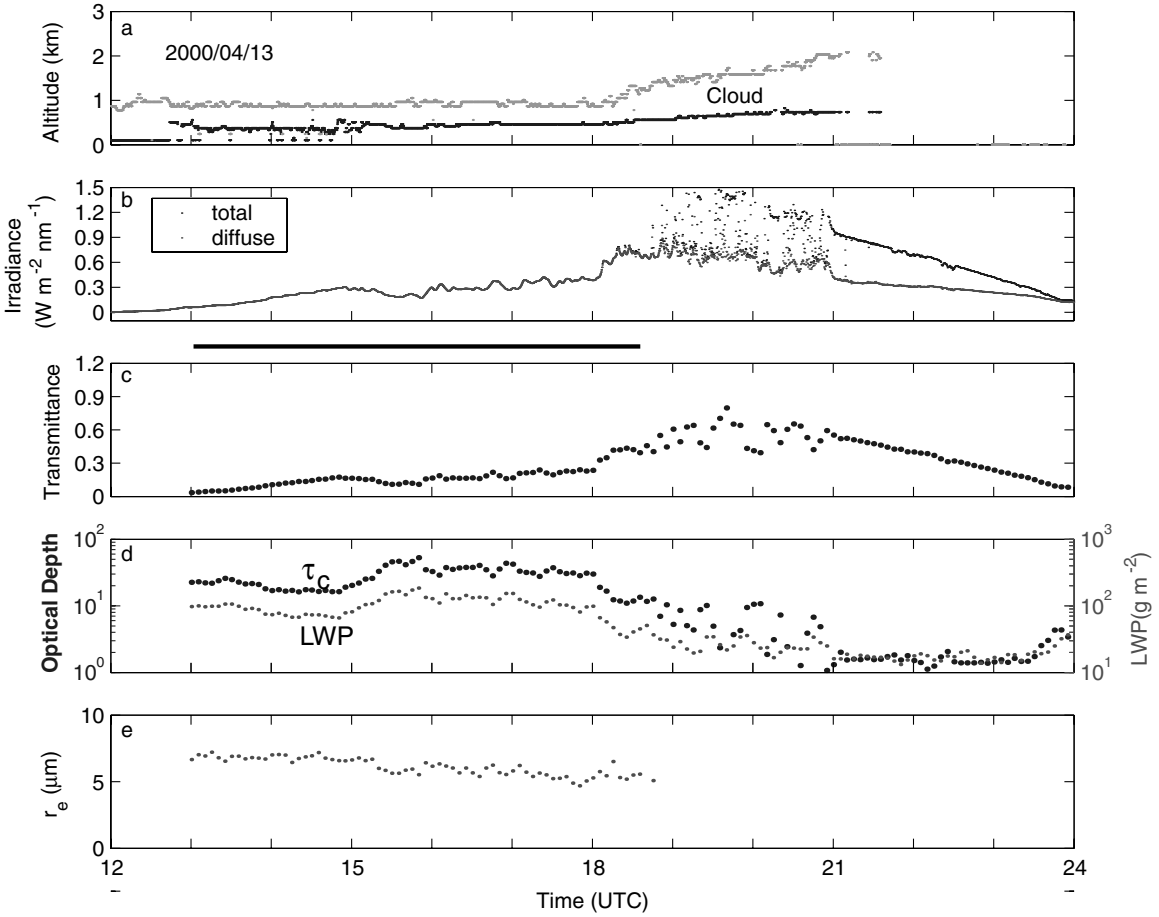

Figure 11. Ground-based remote sensing of cloud microphysical properties. *a*) Time series of cloud-base and cloud-top heights; *b*) total horizontal and diffuse irradiances; *c*) atmospheric transmittance; *d*) cloud optical depth τ_c and liquid water path LWP; and *e*) effective radius of cloud droplets r_e on April 13, 2000 at the U. S. Department of Energy Atmospheric Radiation Measurement site in north central Oklahoma. Black line indicates the period that satisfies requirements for determination of cloud optical depth and effective radius.

As indicated in Figure 11, both LWP and τ_c were found to vary substantially over the course of the day, but the effective radius was remarkably constant. This situation was found to hold on all 13 days in 2000 which met the criteria for application of this method at the measurement site. Thus in ground-based sensing also it is possible to turn the variation in LWP to advantage in inferring r_e; graphs of cloud optical depth versus LWP shown in Figure 12 for the most part exhibit similar linear dependence similar to that seen in the remote sensing work, with slopes that differ substantially from day to day.

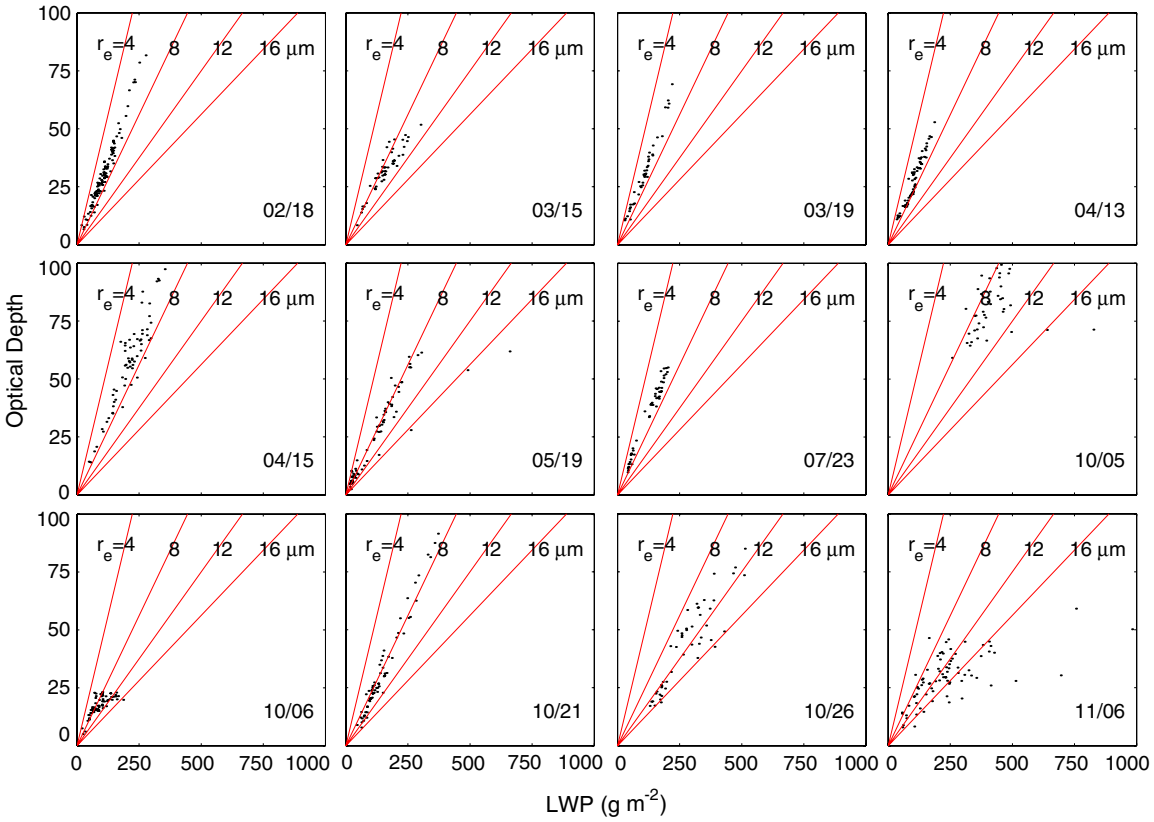

Figure 12. Scatterplots of cloud optical depth (determined from radiometry at 415 nm) against cloud liquid water path determined from microwave radiometry, LWP, at the Atmospheric Radiation Measurement Program site in north central Oklahoma on 12 of 13 days in 2000 that met required conditions of fully overcast sky. Lines denote cloud optical depth for indicated constant values of effective radius, r_e. From Kim *et al*. (2003).

To relate the cloud drop effective radius to aerosol loading we used as a surrogate for that loading measurements of light scattering coefficient σ_{sp} that were made at the surface simultaneously with the remote sensing of the cloud properties. While some correlation was observed in the relation between r_e and σ_{sp} ($R^2 = 0.24$ in a regression of log r_e vs. log σ_{sp}, Figure 13), it is evident that light scattering coefficient at the surface is not a good surrogate for CCN concentration at cloud level and/or that there are additional influences on cloud drop effective radius besides aerosol concentration. One unexplained feature of these results is the remarkable constancy in effective radius despite large variation in both τ_c and LWP. Clearly these questions need to be resolved in future work, but the tools to do this seem at hand, at least from the remote sensing perspective.

As was found in the satellite remote sensing studies, although the dominant influence on cloud albedo was LWP, as expected, there is a substantial day-to-day difference in this dependence that is associated with r_e, Figure 14, and is thus putatively associated with aerosol loading. This influence on cloud albedo also translates into a radiative forcing; for solar zenith angle 60° and LWP = 100 g m^{-2}, as effective radius decreases from 10.2 to 5.8 µm, as determined on different days, the resultant decrease in calculated net shortwave irradiance at the top of the atmosphere (Twomey forcing) is about 50 W m^{-2}.

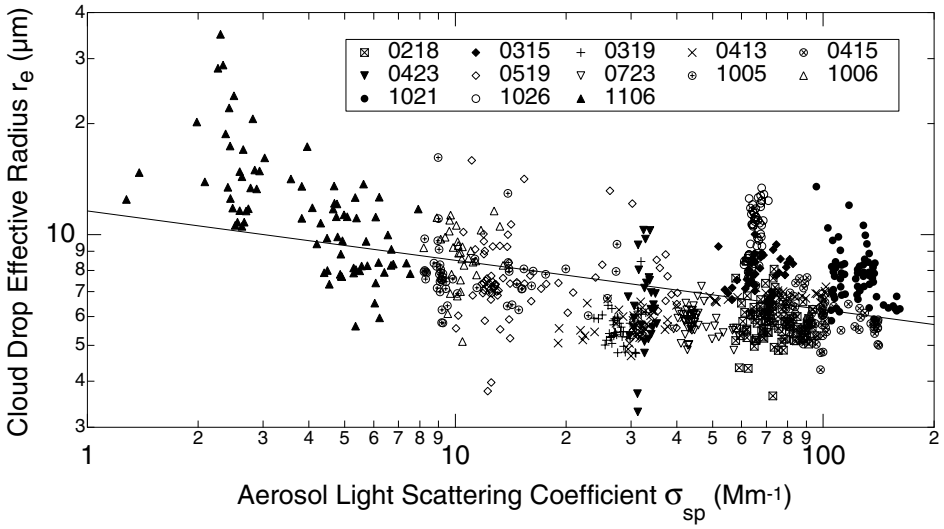

Figure 13. Scatterplot (logarithmic axes) of 5-minute average cloud-drop effective radius r_e vs. light scattering coefficient for submicrometer aerosol at 550 nm σ_{sp}. Data for individual days are distinguished by symbol. Equation of regression is $\log r_e = 1.06 - 0.13 \log\sigma_{sp}$; $R^2 = 0.24$. Data for σ_{sp} are interpolated to measurement time of r_e, and gaps in σ_{sp} (but not r_e) are filled by interpolation. From Kim *et al.* (2003).

QUANTIFYING INDIRECT FORCING BY PROCESS MODELING

The ability of an aerosol particle to serve as a cloud condensation nucleus and thereby increase the number concentration of cloud drops and thus exert an indirect radiative forcing depends on its size and composition and on the supersaturation history that the particle will experience. This history depends not only on the imposed supersaturation governed by water vapor, temperature and mean and turbulent velocities of the air parcel in which the particle finds itself but also on the concentration of other aerosol particles in the vicinity of the particle and their activation spectra. Representing aerosol indirect forcing in climate models thus requires representing the entire life cycle of aerosol particles that might serve as CCN (or that might not): emission of particles, with specification of composition and size, and gaseous precursors; new particle formation in the atmosphere; evolution of the size distribution and composition by coagulation, uptake of condensable gases, and exchange and possible reaction of volatile gases; exchange of water vapor; activation to form cloud droplets; aqueous-phase

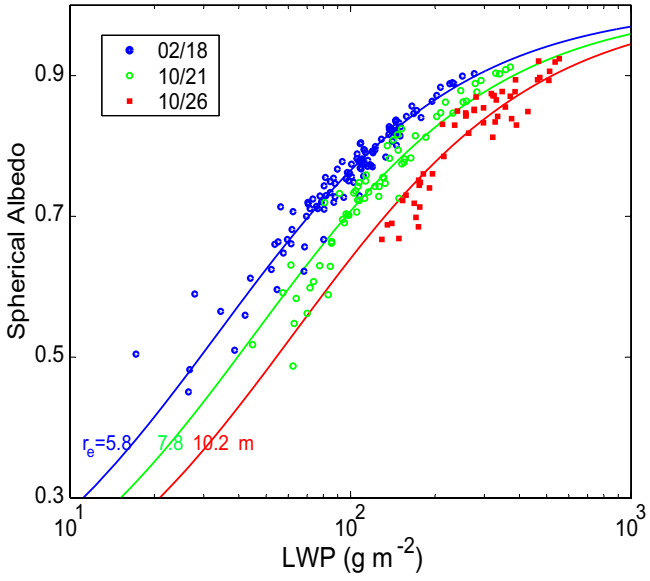

Figure 14. Cloud top spherical albedo as a function of cloud liquid water path, LWP, calculated for measured LWP and optical depth at the Atmospheric Radiation Measurement site in North Central Oklahoma on February 18, October 21, and October 26, 2000. Curves denote cloud albedo for indicated constant values of effective radius, r_e. From Kim *et al.* (2003).

reaction in cloud droplets; in-cloud coagulation; gravitational fall of hydrometeors, cloud dissipation by precipitation and evaporation, and removal of aerosol particles and precursors from the atmosphere by dry and wet deposition. All of these processes must be modeled as a function of location and time, and the pertinent three-dimensional transport processes must also be modeled. Finally, these processes must be represented in climate models as opposed simply to forcing the climate model with an aerosol field calculated off line, for if the aerosol influences on climate are substantial, then the resultant climate modification must be accounted for in the climate model calculation, for example, changes in radiation affecting the thermal structure of the atmosphere and clouds, or increased cloud lifetime and displaced precipitation.

The aerosol properties and the processes governing them required to model the influence of anthropogenic aerosols on cloud microphysical properties and the resultant radiative forcing are summarized in Table 1. Calculation of indirect aerosol forcing of climate change requires knowledge of the anthropogenic enhancement for all properties and processes as well as of the interactions among the several aerosol substances, for example in uptake of volatile gases affecting new particle formation and the uptake of water affecting cloud droplet activation. The indirect forcing is highly nonlinear; thus at a given cloud optical depth, the higher the initial CDNC, the lower the forcing that would result from a given increase in CDNC. This results, for example, in a strong dependence of the forcing by anthropogenic sulfate on the natural abundance of sea salt aerosol. All quantities and processes must be known as a function of location $\boldsymbol{x}$ (2- or 3-dimensional) and time t. Optical properties and changes in radiative fluxes must be known as a function of wavelength λ. There are substantial gaps in understanding of numerous aspects of these processes, for well specified conditions, in addition to the uncertainties attendant on the conditions in the actual atmosphere; there is uncertainty as well in the ability to represent even known understanding in models. To date no satisfactory analysis has been conducted of the uncertainties associated with present knowledge of these processes. Thus it would seem that estimates such as that by Penner *et al*. (2001, Table 5.15), which suggests the forcing due to the first indirect effect of sulfate aerosols as -1.4 W m^{-2}, with a 2/3 uncertainty range from 0 to -2.8 W m^{-2} must be considered rudimentary at best.

Of course aerosol properties and influences must be represented in some statistically meaningful sense. It is not possible, nor should it be set up as a requirement, to model the fate

TABLE 1. Quantities and processes pertinent to description aerosol indirect forcing of climate change and the quantities on which their dependence must be known.

Quantity/Process	Symbol	Dependence on
Particle and gaseous precursor emissions	$e(\boldsymbol{x}, t, r_{ap}, \chi)$	Radius r_{ap}, composition χ
Transport, chemical reaction, microphysical evolution	↓	Concentrations of precursors and other reagents, solar intensity; size dependent concentrations of other aerosol species; 3-D winds, clouds . . .
Aerosol particle number concentration	$n_{ap}(\boldsymbol{x}, t, r_{ap}, \chi)$	Radius, composition
Supersaturation spectrum	$n_{ccn}(s)$	Radius, composition, supersaturation$s$
Cloud formation and dissipation	↓	$n_{ccn}(s)$, updraft velocity, turbulent intensity, precipitation development, heating rate, entrainment . . .
Cloud drop number concentration and properties	$n_{cd}(\boldsymbol{x}, t, r_{cd}, \omega(\lambda))$	Radius, single scatter albedo ω, wavelength λ
Cloud optics	↓	Cloud drop size distribution, Mie scattering
Cloud drop scattering and absorption coefficients	$\{\sigma_{sc}, \sigma_{ac}\}(\boldsymbol{x}, t, \lambda)$	Absorption by dissolved and suspended materials
Vertical integral	↓	Updrafts, entrainment
Cloud scattering and absorption optical depth	$\{\tau_{sc}, \tau_{ac}\}(\boldsymbol{x}, t, \lambda)$	Cloud physical depth, liquid water path
Radiation transfer (3D)	↓	Cloud geometry, surface reflectance
Net spectral flux at top of atmosphere	$F_{toa}(\boldsymbol{x}, t, \lambda)$	

of every individual particle. Rather techniques should be developed to model the pertinent *aerosol* properties–that is properties of the suspension. How this will play out remains to be seen. Much emphasis is currently being given to attempting to represent the size distribution typically by some sort of sectional approach, with the number of prognostic variables being of order 50 (*e.g.*, Korhonen *et al.*, 2004), perhaps with the expectation that computational power will continue grow exponentially (Moore, 1965) to keep up with the computational requirements of representing such a high dimensionality in chemical transport models or climate models. However it would seem that alternative approaches, such as moment based representations (Yu *et al.*, 2003) may offer advantages as they are readily expandable into two or more dimensions (*e.g.*, size and composition) such that computational requirements scale as the sum of a small number of variables (typically 6 or fewer) characterizing each dimension rather than as the product of a considerably greater number of variables in each dimension. Moment methods may be readily combined with statistical approaches such as principal components analysis, which also work with moments, allowing optimized variable selection and coordinate number reduction for highly multivariate problems (Yoon and McGraw, 2004 *a,b*).

The consequences of the uncertainty in indirect forcing are quite substantial in the context of interpretation of global climate change over the industrial period, from the perspective either of empirical interpretation of climate sensitivity from knowledge of the forcing and temperature change over the industrial period (Gregory *et al.*, 2002) or of evaluation of the performance of climate models in representing climate change over this period. As an example one might note the study of Kiehl *et al.* (2000) who used the output of a chemical transport model for sulfate mass as the basis of a calculation of direct and indirect forcing by this aerosol. Shown in Figure 15 is the geographical distribution of the total forcing (preindustrial to present) due to changes in CO_2 and other long-lived greenhouse gases, ozone, and sulfate aerosol, calculated from the geographical distributions of the concentrations. The incremental sulfate concentration field was the same for both calculations, with global average burden 0.74 mg m^{-2} (preindustrial) and 2.97 mg m^{-2}. The difference between the calculations was entirely in the assumed relation between CDNC and sulfate mass concentration, both of which are consistent with recent empirical correlations. The geographical pattern of the total forcing is qualitatively different in the two calculations, and the global mean total forcing differs by more

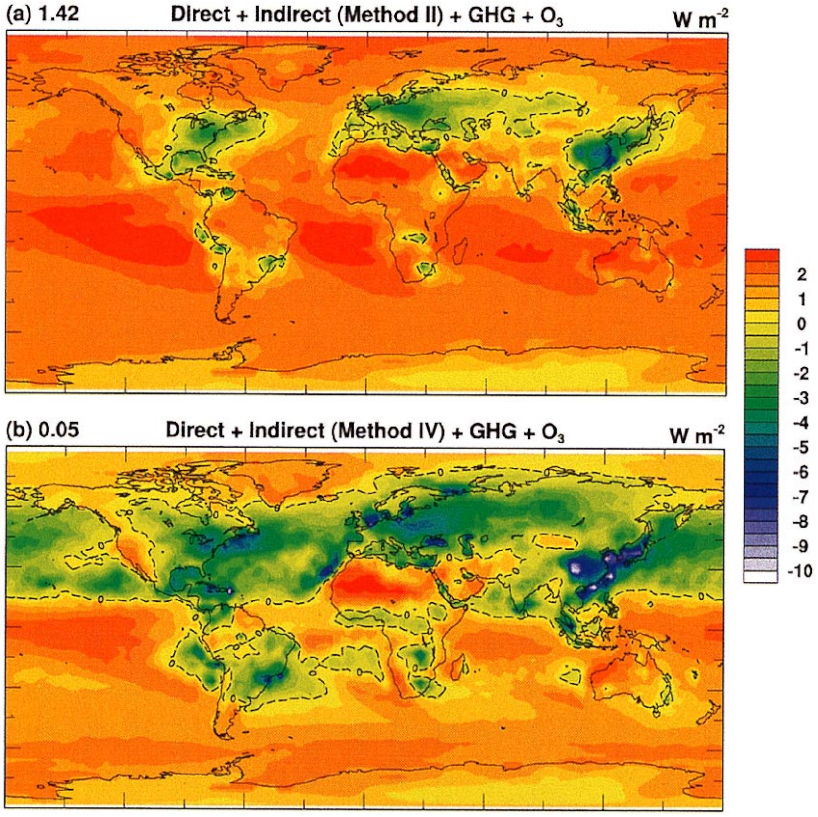

Figure 15. Global average (at upper left of each panel) and geographical distribution of annual-average radiative forcing of climate change due to enhanced concentrations of long-lived greenhouse gases, ozone, and sulfate aerosol (direct and first indirect forcing only). The two panels present results for sulfate indirect forcing calculated by two different relations between cloud drop number concentration and sulfate concentration. Dashed contour (0) demarcates regions of positive and negative forcing. From Kiehl *et al.* (2000).

than a factor of 25, from a very small 0.05 W m^{-2} to a much more appreciable 1.42 W m^{-2} (indirect sulfate aerosol forcing 1.78 W m^{-2} and 0.42 W m^{-2}, respectively). This comparison acutely illustrates the consequences of the present latitude in calculation of radiative forcing over the industrial period due to uncertainty in aerosol indirect forcing.

CONCLUSIONS

There is now abundant evidence of the importance of aerosol indirect forcing of climate change in the context of anthropogenic forcings over the industrial period. However this forcing remains highly uncertain. So far it has proved difficult to quantify the indirect forcing of anthropogenic aerosols on global scales, by satellite or other remote sensing measurements. Likewise, there are many barriers remaining to developing understanding and model-based representation of this forcing. For example, even though the principles of cloud drop activation seem well understood based on classic Köhler theory, it has proved difficult to quantitatively relate the number concentration of aerosol particles or the number spectrum of CCN as a function of supersaturation to the number concentration of cloud drops in actual clouds. This understanding is but one of many essential components of any effort to represent indirect aerosol forcing in climate models.

In its 2001 assessment of the several forcings of climate change the Intergovernmental Panel on Climate Change characterized the level of scientific understanding of the aerosol indirect forcing as "very low." Perhaps it would be more accurately stated that although there have been substantial increases in understanding this forcing, the ability to quantify it remains very low and will continue to remain very low unless and until much more effort is directed to observationally quantifying it and to understanding the governing processes.

Acknowledgments

I am indebted to numerous colleagues at Brookhaven National Laboratory and elsewhere for their contributions to the research in our group, some of which is presented here, especially Carmen Benkovitz, Robert McGraw, Byung-Gon Kim, and Harshvardhan (Purdue University). This research was supported by the Climate Change Research Division of the U.S. Department of Energy (DOE) and was performed under the auspices of DOE under Contract No. DE-AC02-98CH10886.

References

Albrecht B. A. Aerosols, cloud microphysics, and fractional cloudiness. *Science* **245**, 1227-1230 (1989).

Benkovitz C. M., Berkowitz C. M., Easter R. C., Nemesure S., Wagener R. and Schwartz S. E. Sulfate over the North Atlantic and adjacent continental regions: Evaluation for October and November 1986 using a three-dimensional model driven by observation-derived meteorology. *J. Geophys. Res.* **99**, 20725-20756 (1994).

Benkovitz C. M., Miller M. A., Schwartz S. E. and Kwon O-U. Dynamical influences on the distribution and loading of SO2 and sulfate over North America, the North Atlantic and Europe in April 1987. *Geochem. Geophys. Geosyst.* **2**, Paper 2000GC000129 (2001). http://www.agu.org/journals/gc/gc0106/2000GC000129/zfs2000GC000129.html .

Boucher O. and Haywood J. On summing the components of radiative forcing of climate change. *Climate Dynamics* **18**, 297-302 (2001).

Bréon F. M., Tanré D., and Generoso S. Aerosol effect on cloud droplet size monitored from satellite. *Science* **295**, 834-838 (2002).

Chameides W. L., Luo C., Saylor R., Streets D., Huang Y., Bergin M., and Giorgi F. Correlation between model-calculated anthropogenic aerosols and satellite-derived cloud optical depths: Indication of indirect effect? *J. Geophys. Res.*, **107**, doi: 10.1029/2000JD000208 (2002).

Charlson R. J., Schwartz S. E., Hales J. M., Cess R. D., Coakley J. A., Jr., Hansen J. E. and Hofmann D. J. Climate forcing by anthropogenic aerosols. *Science* **255**, 423-430 (1992).

Chuang, P. Y., D. R. Collins, H. Pawlowska, J. R. Snider, H. H. Jonsson, J. L. Brenguier, R. C. Flagan, and J. H. Seinfeld, CCN Measurements during ACE-2 and their Relationship to Cloud Microphysical Properties, *Tellus* **52B**, 843-857 (2000).

Dong, X., T. P. Ackerman, E. E. Clothiaux, P. Pilewskie, and Y. Han, Microphysical and radiative properties of boundary layer stratiform clouds deduced from ground-based measurements. *J. Geophys. Res*., **102**, 23829-23843 (1997).

Feingold, G., W. Eberhard, D. E. Lane, and M. Previdi, First measurements of the Twomey effect using ground-based remote sensors, *Geophys. Res. Lett.* **30**, 1287, doi: 10.1029/2002GL016633 (2003).

Folland, C. K. *et al*. "Observed climate variability and change," in IPCC (2001), pp. 99-181.

Gregory, J. M., R. J. Stouffer, S. C. B. Raper, P. A. Stott and N. A. Rayner: An Observationally based estimate of the climate sensitivity. *J. Climate* **15**, 3117-3121 (2002).

Han Q., Rossow W. B. and Lacis A. A. Near-global survey of effective droplet radii in liquid water clouds using ISCCP data. *J. Climate* **7**, 465-497 (1994).

Han, Q. Y., W. B. Rossow, J. Chou, and R. M. Welch. Global survey of the relationship of cloud albedo and liquid water path with droplet size using ISCCP. *J. Climate* **11**, 1516-1528 (1998).

Han, Q. Y., W. B. Rossow, J. Zeng, and R. M. Welch. Three different behaviors of liquid water path of water clouds in aerosol-cloud interactions. *J. Atmos. Sci.* **59**, 726-735 (2002) .

Hansen J. E. and Travis L. D., Light-scattering in planetary atmospheres. *Space Sci. Rev.* **16,** 527-610 (1974).

Harshvardhan, Schwartz S. E., Benkovitz C. M. and Guo G. Aerosol influence on cloud microphysics examined by satellite measurements and chemical transport modeling. *J. Atmos. Sci*. **59**, 714-725 (2002).

Intergovernmental Panel on Climate Change (IPCC). *Climate Change 2001: The Scientific Basis. Contribution of Working Group I to the Third Assessment Report of the Intergovernmental Panel on Climate Change,* Edited by Houghton, J. T. *et al*., Cambridge: Cambridge University Press, 2001.

Kiehl J. T. and Trenberth K. E. Earth's annual global mean energy budget. *Bull. Amer. Meteorol. Soc*. **78**, 197-208 (1997),.

Kiehl J. T., T. L. Schneider, P. J. Rasch, M. C. Barth, and J. Wong J. Radiative Forcing due to Sulfate Aerosols from Simulations with the National Center for Atmospheric Research Community Climate Model, Version 3. *J. Geophys, Res*. **105**, 1441-1457 (2000).

Kim B.-G., Schwartz S. E., Miller M. A. and Min Q. Effective radius of cloud droplets by ground-based remote sensing: Relationship to aerosol. *J. Geophys. Res*., **108**, 4740, doi: 10.1029/2003JD003721 (2003).

Korhonen H., Lehtinen K. E. J. and Kulmala M. Multicomponent aerosol dynamics model UHMA: model development and validation. *Atmos. Chem. Phys. Discuss*. **4**, 471–506 (2004). www.atmos-chem-phys.org/acpd/4/471/ .

Leaitch W. R., Strapp J. W., Isaac G. A. and Hudson J. G. Cloud droplet nucleation and cloud scavenging of aerosol sulphate in polluted atmospheres. *Tellus* **38B**, 328-344 (1986).

Liu, Y., and P. H. Daum, Indirect warming effect from dispersion forcing, *Nature* **419**, 580-581 (2002).

Min, Q., and L.C. Harrison, Cloud properties derived from surface MFRSR measurements and comparison with GEOS results at the ARM SGP site, *Geophys. Res. Lett.* **23,** 1641-1644 (1996).

Moore G. E. Cramming more components onto integrated circuits. *Electronics* **38**, (8), 114-117 (1965).

Nakajima T., Higurashi A., Kawamoto, K. and Penner J. E. A possible correlation between satellite-derived cloud and aerosol microphysical parameters. *Geophys. Res. Lett*. **28**, 1171-1174 (2001).

Penner J. E. *et al.* "Aerosols, their direct and indirect effects," in IPCC (2001), pp. 289-348.

Penner J. E., Dong X., and Chen Y. Observational evidence of a change in radiative forcing due to the indirect aerosol effect. *Nature* **427**, 231-234 (2004).

Ramanathan V. The role of earth radiation budget studies in climate and general circulation research. *J. Geophys. Res.* **92**, 4075-4095 (1987).

Ricchiazzi, P., S. Yang, C. Gautier, and D. Sowie, SBDART: A research and teaching software tool for plane-parallel radiative transfer in the Earth's atmosphere, *Bull. Amer. Meteorol. Soc.* **79***,* 2101-2114 (1998).

Schwartz S. E. and Slingo A., "Enhanced shortwave cloud radiative forcing due to anthropogenic aerosols," in *Clouds, Chemistry and Climate–Proceedings of NATO Advanced Research Workshop*, edited by Crutzen P. and Ramanathan V., Heidelberg: Springer, 1996. pp. 191-236.

Schwartz S. E., Harshvardhan, and Benkovitz C. M. Influence of anthropogenic aerosol on cloud optical depth and albedo shown by satellite measurements and chemical transport modeling. *Proc. Natl. Acad. Sci. U.S.A*. **99**, 1784-1789 (2002).

Twomey S. Pollution and planetary albedo. *Atmos. Environ.* **8**, 1251-1256 (1974).

Twomey S. *Atmospheric Aerosols*, New York: Elsevier, 1977.

Vong, R. J. and Covert, D. S. Simultaneous observations of aerosol and cloud droplet size spectra in marine stratocumulus. *J. Atmos. Sci.* **55**, 2180–2192 (1998).

Yoon C. and McGraw R. Representation of generally-mixed multivariate aerosols by the quadrature method of moments: I. Statistical foundation. *J. Aerosol Sci*. in press, 2004.

Yoon C. and McGraw R. Representation of generally-mixed multivariate aerosols by the quadrature method of moments: II. Aerosol dynamics. *J. Aerosol Sci*. in press, 2004.

Yu S., Kasibhatla P. S., Wright D. L., Schwartz S. E., McGraw R. and Deng A. J. Moment-based simulation of microphysical properties of sulfate aerosols in the eastern United States: Model description, evaluation and regional analysis. *J. Geophys Res*., **108** 4353 (2003). doi:10.1029/2002JD002890.